communications materials

ARTICLE

https://doi.org/10.1038/s43246-021-00167-6 OPEN

A unified perturbative approach to electrocaloric effects

Mónica Graf [1] & Jorge Íñiguez [1,2]✉

The electrocaloric effect, that is, the temperature change experienced by an insulator upon application of an electric field, offers promising ecofriendly alternatives to refrigeration. However, the theoretical treatments of this response are mostly case specific and lack a unified picture revealing the similarities and differences among the various known effects. Here, we show that the electrocaloric effect lends itself to a straightforward interpretation when expressed as a Taylor series in the external field. Our formalism explains in a unified and simple way the most notable small-field effects reported in the literature, namely the so-called normal and inverse electrocaloric responses, corresponding to an increase or decrease of temperature under applied field, as usually found in ferroelectrics or antiferroelectrics, respectively. This helps us to clarify their physical interpretation. We then discuss in detail atomistic simulations for the prototype ferroelectric $PbTiO_3$, explicitly evaluating subtle predictions of the theory, such as the occurrence of competing contributions to the electrocaloric response.

[1] Materials Research and Technology Department, Luxembourg Institute of Science and Technology, Esch/Alzette, Luxembourg. [2] Department of Physics and Materials Science, University of Luxembourg, Belvaux, Luxembourg. ✉email: jorge.iniguez@list.lu

An electric field can be used to change the temperature of an insulator, by virtue of the so-called electrocaloric effect. Electrocaloric effects hold the promise of an ecofriendly alternative to refrigeration, one of the most energy-consuming activities today and in the foreseeable future. Electrocaloric effects are strong in ferroelectric and antiferroelectric materials because of their anomalously large dielectric responses and the field-driven phase transitions that can be easily induced near the Curie point[1].

The thermodynamic description of the electrocaloric cooling cycle is well-established[1]. The key step is the adiabatic temperature change, which can be expressed as

$$\begin{aligned}\Delta T(E_\alpha) &= -\int_0^{E_\alpha} \frac{T}{C_{\mathbf{E}}}\left(\frac{\partial S}{\partial E'_\alpha}\right)_T \mathrm{d}E'_\alpha \\ &= -\int_0^{E_\alpha} \frac{T}{C_{\mathbf{E}}}\left(\frac{\partial P_\alpha}{\partial T}\right)_{\mathbf{E}} \mathrm{d}E'_\alpha \\ &= -\int_0^{E_\alpha} \frac{T}{C_{\mathbf{E}}}\pi_\alpha \mathrm{d}E'_\alpha,\end{aligned} \tag{1}$$

where the integral runs from zero to a final electric field E_α, applied along the α Cartesian direction. S, T, and $C_{\mathbf{E}}$ are, respectively, the entropy, temperature, and constant-field heat capacity. P_α is the polarization component conjugate to the applied field E_α, and its T-derivative is the pyroelectric coefficient π_α. Note that we have used the Maxwell relation between the field derivative of the entropy and the pyroelectric vector, which is expected to hold for ergodic materials. (Thus, the formalism introduced here is, in principle, not applicable to relaxor ferroelectrics.) Note also that the repeated α index does not involve an implicit sum; we write this α, on both sides of the equation, to emphasize the fact that the electrocaloric response can be anisotropic.

Also important is the isothermal entropy change

$$\Delta S(E_\alpha) = \int_0^{E_\alpha} \pi_\alpha \mathrm{d}E'_\alpha, \tag{2}$$

which quantifies the amount of heat the electrocaloric material will exchange with the object to be cooled. The product $\Delta T(E_\alpha)\Delta S(E_\alpha)$ is usually taken as the figure of merit for electrocaloric cooling performance.

These expressions are deceivingly simple, as all the quantities in the integrands depend on both field and temperature (itself field-dependent, by virtue of the electrocaloric effect). Further, they may present complex behaviors (in particular, discontinuities) across the field- and temperature-driven phase transitions.

There are well-known strategies to solve these integrals self-consistently[1]; this will not be our focus here. Rather, we want to examine the ingredient that has the greatest influence on the basic features (magnitude and sign) of the electrocaloric temperature and entropy changes, namely, the pyroelectric vector $\boldsymbol{\pi}$. Indeed, $\boldsymbol{\pi}$ fully determines $\Delta S(E_\alpha)$; further, of the quantities contributing to $\Delta T(E_\alpha)$, $\boldsymbol{\pi}$ is likely to be the most sensitive to an electric field and, more importantly, it is the only one whose sign is not defined. (Both T and C_E are always positive.)

Interestingly, we can rewrite Eq. (1) in differential form as

$$\frac{\mathrm{d}T(E_\alpha)}{\mathrm{d}E_\alpha} = -\frac{T}{C_{\mathbf{E}}}\left(\frac{\partial S}{\partial E_\alpha}\right)_T. \tag{3}$$

This expression is the basis for the physical interpretation of electrocaloric effects[1]. For example, it is experimentally observed that, in ferroelectrics, the application of an electric field usually results in a positive temperature change, which is attributed to the fact that electric fields create order (reduce the entropy) in such systems[1]. In contrast, negative values of ΔT have been observed in antiferroelectrics[2–5], or when a field is applied perpendicular to the polarization of a ferroelectric phase[6], which is compatible with the intuitive notion that, in such cases, the electric field will destabilize the equilibrium state and cause disorder (increase the entropy). These diverse observations have been reproduced by atomistic simulations[7–13] and explained by the corresponding Landau phenomenological theories[1,2,12,14], suggesting that we understand electrocaloric effects quite well.

However, we think the situation is not fully satisfactory, for one main reason: The theoretical treatments in the literature are case-specific, and we lack a unified and simple picture revealing the similarities and differences among the various known effects. Also, we find that, while intuitively appealing, some frequent assumptions (i.e., that electric fields cause disorder in antiferroelectrics) are somewhat vague, and we miss a formalism that allows us to interpret the observed behaviors (and eventually think about new ones) in a more rigorous manner. Here, we provide such a formalism, and show how it helps us to rationalize all the (small-field) electrocaloric effects observed in the literature. Further, we show the results of atomistic simulations that allow us to explicitly evaluate intriguing predictions of the theory, such as the existence of competing contributions to the electrocaloric response.

Results

Formal considerations. Let us focus on how π_α controls $\Delta T(E_\alpha)$. For the sake of simplicity, we work with an approximate version of the adiabatic temperature change

$$\Delta T(E_\alpha) \approx -\frac{T^{(0)}}{C_{\mathbf{E}}^{(0)}}\int_0^{E_\alpha} \pi_\alpha(T^{(0)})\,\mathrm{d}E'_\alpha, \tag{4}$$

where the "(0)" superscript marks values evaluated at zero applied field and at the zero-field temperature $T^{(0)}$. Thus, this approximate expression captures the electrocaloric effect as obtained when we neglect the field dependence of T and $C_{\mathbf{E}}$, as well as the variation of π_α and $C_{\mathbf{E}}$ caused by electrocaloric heating or cooling; these are common approximations in the electrocaloric literature. (Unless we work at low temperatures, we can safely assume $|\Delta T(E_\alpha)| \ll T^{(0)}$, as the largest measured electrocaloric effects are typically below 20 K[15]. Also, we can expect relatively small variations in $C_{\mathbf{E}}$ except in the close vicinity of phase transitions; more on this below.)

Let us examine Eq. (4) analytically. We start by writing $\mathbf{P}$ as a Taylor series in $\mathbf{E}$,

$$P_\mu = P_\mu^{(0)} + \epsilon_0 \sum_\beta \chi_{\mu\beta}^{(0)} E_\beta + \epsilon_0 \sum_{\beta\gamma} \chi_{\mu\beta\gamma}^{(1)} E_\beta E_\gamma + \ldots, \tag{5}$$

where $\mathbf{P}^{(0)}$ is the spontaneous polarization, $\boldsymbol{\chi}^{(n)}$ is the nth-order dielectric susceptibility tensor, and ϵ_0 is the vacuum permittivity. For convenience, we work with a Cartesian coordinate system with one axis parallel to α, the direction of the applied field. Hence, we have $E_\beta = \delta_{\beta\alpha}E_\alpha$, where $\delta_{\beta\alpha}$ is the Kronecker delta; we thus obtain the α component of the polarization as

$$P_\alpha = P_\alpha^{(0)} + \epsilon_0 \chi_{\alpha\alpha}^{(0)} E_\alpha + \epsilon_0 \chi_{\alpha\alpha\alpha}^{(1)} E_\alpha^2 + \ldots, \tag{6}$$

where only the α-diagonal tensor elements appear. This expression for P_α is general and can be used to describe any phase of an insulating material, be it ferroelectric, antiferroelectric, paraelectric, or simply dielectric. Also, note that the dielectric tensors in the above equations describe the properties of a single crystal with a well-defined orientation with respect to our Cartesian setting.

By taking the T-derivative of Eq. (6) at constant field, we obtain

$$\pi_\alpha = \pi_\alpha^{(0)} + \pi_{\alpha\alpha}^{(1)} E_\alpha + \pi_{\alpha\alpha\alpha}^{(2)} E_\alpha^2 + \ldots, \tag{7}$$

Table 1 Expected electrocaloric effects.

Case, $\mathbf{P}^{(0)}$	E	$\Delta T^{(1)}(E_\alpha)$	$\Delta T^{(2)}(E_\alpha)$	exp.
PE ($T > T_C$) $\mathbf{P}^{(0)} = \mathbf{0}$	any	0	> 0	> 0
AFE ($T < T_C$) $\mathbf{P}^{(0)} = \mathbf{0}$	any	0	< 0	< 0
FE ($T < T_C$) $(0, 0, P_z^{(0)} > 0)$	E_x	0	< 0	< 0
	$E_z > 0$	> 0	< 0	> 0
	$E_z < 0$	< 0	< 0	< 0

The Table includes the paraelectric (PE), ferroelectric (FE), and antiferroelectric (AFE) states. Shown are the expected signs of the linear and quadratic contributions to $\Delta T(E\alpha)$ ($\Delta T^{(1)}(E\alpha)$ and $\Delta T^{(2)}(E\alpha)$ columns, see text), as well as the sign of the experimentally measured ΔT ("exp." column).

where the $\boldsymbol{\pi}^{(0)}$ vector captures the T-dependence of the spontaneous polarization $\mathbf{P}^{(0)}$. For $n \geq 1$, the $\boldsymbol{\pi}^{(n)}$ tensors account for the field-induced pyroelectric effect, with

$$\boldsymbol{\pi}^{(n)} = \epsilon_0 \left(\frac{\partial \boldsymbol{\chi}^{(n-1)}}{\partial T} \right)_{\mathbf{E}}, \tag{8}$$

where the pyroelectric tensor of nth-order in the field series depends on the susceptibility of $(n-1)$th-order. Using Eq. (7), we resolve Eq. (4) and obtain

$$\begin{aligned} \Delta T(E_\alpha) \approx & -\frac{T^{(0)}}{C_E^{(0)}} \left(\pi_\alpha^{(0)} E_\alpha + \frac{1}{2} \pi_{\alpha\alpha}^{(1)} E_\alpha^2 + \frac{1}{3} \pi_{\alpha\alpha\alpha}^{(2)} E_\alpha^3 + \ldots \right) \\ = & \ \Delta T^{(1)}(E_\alpha) + \Delta T^{(2)}(E_\alpha) + \Delta T^{(3)}(E_\alpha) + \ldots, \end{aligned} \tag{9}$$

where we define $\Delta T^{(n)}(E_\alpha)$ as the nth-order contribution to the adiabatic temperature change. Also, here it is implicitly assumed that the pyroelectric coefficients are evaluated at $T^{(0)}$. Let us now see how this expression allows us to understand all the known electrocaloric effects in ferroelectric and antiferroelectric compounds for small applied electric fields. Our conclusions are summarized in Table 1.

For the sake of concreteness, here we discuss ferroelectric and antiferroelectric materials with an isotropic (e.g., cubic) high-temperature paraelectric phase, as is the case of perovskite oxides (e.g., $PbTiO_3$ or $PbZrO_3$), noting that our arguments can be generalized.

Let us begin by discussing the electrocaloric response above the Curie temperature (T_C) for a material that can be either ferroelectric or antiferroelectric. In this case, we do not have any spontaneous polarization ($\mathbf{P}^{(0)} = \boldsymbol{\pi}^{(0)} = \mathbf{0}$); hence, $\Delta T(E_\alpha) \approx \Delta T^{(2)}(E_\alpha)$, which is dominated by the lowest-order field-induced pyroelectric effect, $\boldsymbol{\pi}^{(1)}$. As we know from Eq. (8), $\boldsymbol{\pi}^{(1)}$ is just the T-derivative of the linear dielectric susceptibility $\boldsymbol{\chi}^{(0)}$.

As it is well-known, both ferroelectric and antiferroelectric phase transitions are characterized by a dielectric anomaly at zero field, i.e., a maximum of $\boldsymbol{\chi}^{(0)}$ at T_C. To fix ideas, we can imagine that all the diagonal components of $\boldsymbol{\chi}^{(0)}$ follow a Curie–Weiss law approximately. (Our simulation results for $PbTiO_3$—see Fig. 1—are a representative case.) This maximum controls the T-dependence of $\boldsymbol{\chi}^{(0)}$ in a wide range around T_C, yielding $\pi_{\alpha\alpha}^{(1)} > 0$ for $T < T_C$ and $\pi_{\alpha\alpha}^{(1)} < 0$ for $T > T_C$. Hence, in particular, the paraelectric phase of all ferroelectrics and antiferroelectrics is characterized by $\pi_{\alpha\alpha}^{(1)} < 0$; according to Eq. (9), this should result in $\Delta T(E_\alpha) > 0$ for all α directions, as it is indeed observed.

Interestingly, the situation is rather similar for an antiferroelectric state: we still have $\mathbf{P}^{(0)} = \boldsymbol{\pi}^{(0)} = \mathbf{0}$ and $\Delta T(E_\alpha) \approx \Delta T^{(2)}(E_\alpha) \propto \pi_{\alpha\alpha}^{(1)}$. However, now we have $T < T_C$ and, as mentioned above, $\pi_{\alpha\alpha}^{(1)} > 0$. Hence, we expect $\Delta T(E_\alpha) < 0$, in agreement with the experimental observations.

Note that in all the above cases the electrocaloric temperature change does not depend on the sign of the applied field, a feature that is expected from the symmetry of paraelectric and antiferroelectric states, and which we readily obtain from our formalism.

Suppose now that we are in a ferroelectric phase. Without loss of generality, we assume that $\mathbf{P}^{(0)}$ is parallel to the z Cartesian direction, with $P_z^{(0)} > 0$ and $P_x^{(0)} = P_y^{(0)} = 0$. In this case, the $\boldsymbol{\pi}^{(0)}$ vector has one nonzero component ($\pi_z^{(0)} < 0$) and two null ones ($\pi_x^{(0)} = \pi_y^{(0)} = 0$). Further, we have $\pi_{\alpha\alpha}^{(1)} > 0$ for all α (from the Curie–Weiss law and the fact that $T < T_C$).

Let us imagine we apply a field E_x along the x Cartesian direction, thus perpendicular to $\mathbf{P}^{(0)}$. This case is exactly analogous to the antiferroelectric state discussed above: according to Eq. (9), the response is controlled by $\pi_{xx}^{(1)} > 0$. Hence, exactly as in the antiferroelectric state, we expect an inverse electrocaloric response with $\Delta T(E_x) < 0$, an experimentally observed behavior that might seem surprising[6,16], but is readily obtained and explained within our formalism.

Finally, suppose that we apply a field along z, the direction of the spontaneous polarization. Here, for the first time in this discussion, we have a nonzero linear contribution to the adiabatic temperature change, and we can write $\Delta T(E_z) \approx \Delta T^{(1)}(E_z) + \Delta T^{(2)}(E_z)$.

Concerning $\Delta T^{(2)}(E_z)$, the situation is identical to the above cases for $T < T_C$: it is dominated by $\pi_{zz}^{(1)} > 0$, which yields $\Delta T^{(2)}(E_z) < 0$ regardless of the sign of the applied field E_z.

In contrast, the linear contribution does depend on whether E_z is parallel or antiparallel to spontaneous polarization. Further, $\Delta T^{(1)}(E_z)$ is proportional to $\pi_z^{(0)}$, which is negative when $P_z^{(0)} > 0$. Hence, we have: $\Delta T^{(1)}(E_z) > 0$ for a parallel field ($E_z > 0$), and $\Delta T^{(1)}(E_z) < 0$ when the field goes against P_z.

Thus, we have two qualitatively different cases. If the applied field goes against the polarization, $\Delta T^{(1)}(E_z)$ and $\Delta T^{(2)}(E_z)$ are both negative, and we have every reason to expect $\Delta T(E_z) < 0$. However, for fields parallel to polarization, we have a competition between the linear and quadratic contributions to $\Delta T(E_z)$, and the net result is in principle undetermined. Interestingly, experimental studies of ferroelectric phases show – without exception, as far as we know —that the temperature change is positive for fields parallel to the spontaneous polarization[1], and negative for fields tending to reverse it[6,17,18]. This is in agreement with the expectations from our formalism, suggesting that, for the case of parallel fields, the linear effect ($\Delta T^{(1)}(E_z) \propto \pi_z^{(0)} E_z > 0$) dominates over the quadratic one ($\Delta T^{(2)}(E_z) \propto \pi_{zz}^{(1)} E_z^2 < 0$).

Hence, as summarized in Table 1, we find that, in all the cases considered, the leading nonzero contribution to $\Delta T(E_\alpha)$ agrees in sign with the adiabatic temperature change observed experimentally for relatively small applied fields. We should note that the formalism just introduced bears obvious similarities with previously proposed theories to discuss electrocaloric effects, e.g., in the context of antiferroelectrics[2,9]. The novelty here relies on the fact that our equations are general and can be applied to any material and phase (ferroelectric, antiferroelectric, paraelectric, or simply dielectric), revealing the way they are connected and evidencing the (somewhat trivial) origin of the so-called inverse effects. Our formalism also emphasizes that the basic electrocaloric response (i.e., the sign of the T-change) can be understood from simple universal arguments, not relying on specific atomistic or phenomenological models.

Numerical results. To gain further insight, and to evaluate the accuracy of low-order approximations to $\Delta T(E_\alpha)$, we now compute explicitly the $\Delta T^{(n)}(E_\alpha)$ terms in Eq. (9) for prototype compound $PbTiO_3$ (PTO).

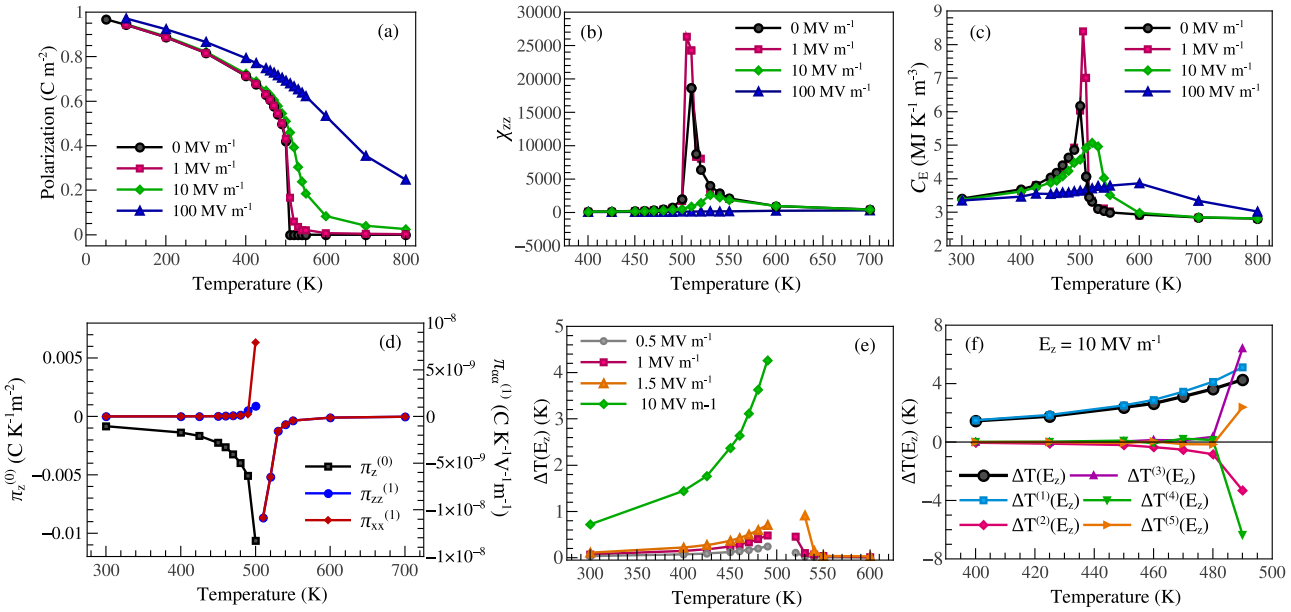

Fig. 1 Simulation results for $PbTiO_3$. We show the temperature and field dependence of **P** (**a**), χ (**b**), and specific heat C_E (**c**). **d** shows the T-dependence of the $\pi_z^{(0)}$, $\pi_{xx}^{(1)}$, and $\pi_{zz}^{(1)}$ components of the pyroelectric tensors; they correspond to the case in which we have a positive spontaneous polarization along z, as discussed in the text. Also shown is $\Delta T(E_z)$ obtained for different electric fields (**e**), as well as the result for $E_z = 10$ MV m^{-1} decomposed in the different $\Delta T^{(n)}(E_z)$ contributions (**f**). **a**–**c** Different colors and symbols are used to represent different values of the applied electric field (black circles for zero field, etc.). **d** Different colors and symbols correspond to different tensor components (black squares for $\pi_z^{(0)}$, etc.). **e** Different colors and symbols correspond to different electric fields (gray circles for 0.5 MV m^{-1}, etc.). **f** Different colors and symbols correspond to different orders in the applied field (black circles for the total temperature change, blue squares for the term that depends linearly on the field, etc.). **e**, **f** No results are shown for $T \gtrsim T_C$ whenever the applied **E** induces a transition.

We simulate PTO using the so-called second-principles methods introduced in refs. [19] and [20], i.e., atomistic model potentials with all parameters fitted from first principles and whose accuracy can be systematically improved (see "Methods"). More precisely, we use the model potential first introduced in ref. [19], which has proven its accuracy in reproducing the basic ferroelectric behavior of the material as well as many subtle structural features, as e.g., related to its domain walls[21,22]. Let us stress that, in these simulations, all the degrees of freedom for the lattice (i.e., all atomic positions, all strains) are treated on equal footing; hence, our calculations include all contributions to the electrocaloric response, and there is in fact no easy way to differentiate them in the manner is often done in phenomenological Landau approaches (where it is natural to distinguish the "dipole" subsystem from the "phonon" bath[1]). Finally, let us mention that the only noteworthy deficiency of our second-principles model pertains to the predicted T_C, which is lower than the experimental one (510 K vs 760 K), but this is not critical for the present purposes.

We solve our PTO model as a function of temperature and applied electric field[19] by running Monte Carlo simulations, using periodically repeated supercells composed of $10 \times 10 \times 10$ or $12 \times 12 \times 12$ elemental perovskite units. (Larger cells are considered in the proximity of T_C.) At a given T, we run 10,000 Monte Carlo sweeps for thermalization, followed by 75,000 to 100,000 sweeps to compute averages. We checked that these calculation conditions yield sufficiently accurate results.

The key quantities we monitor are the equilibrium polarization **P**, the dielectric susceptibility χ, the pyroelectric vector π, and the specific heat C_E, which we compute using standard linear-response formulas[23]. (The formulas used here are given in the Methods section; they closely resemble the ones employed in other studies of electrocaloric effects by Monte Carlo simulations, e.g., in refs. [12,14].) We can thus compute the Taylor series for π (Eq. (7)) and for $\Delta T(E_\alpha)$ (Eq. (9)). (In "Methods" and Supplementary Figs. 1, 2, and 3 we give extra details on the calculation of the $\Delta T^{(n)}(E_\alpha)$ contributions.) Our results are summarized in Fig. 1.

We obtain a ferroelectric phase transition at $T_C = 510$ K (Fig. 1a), marked by a near divergence of the susceptibility (Fig. 1b); this is characteristic of a weakly first-order transformation and is in qualitative agreement with the experimental result[24]. Without loss of generality, we choose $\mathbf{P}^{(0)} = (0, 0, P_z^{(0)})$, with $P_z^{(0)} > 0$ below T_C. Of note is the qualitative change of the phase transition as we apply an electric field: for the small applied field, the susceptibility peak reaches higher values, reflecting the fact that the transition becomes more continuous (for a discussion of this kind of effect, see, e.g., refs. [25] and [26]); for larger fields, the transition becomes diffuse and the related anomalies in the susceptibility (Fig. 1b) and heat capacity (Fig. 1c) tend to disappear.

For clarity, Fig. 1b only shows the temperature and field dependence of one susceptibility component, χ_{zz}. However, note that, by symmetry, the χ tensor only has diagonal components; further, for $T > T_C$ they are all equal (cubic phase), while for $T < T_C$ we have $\chi_{xx} = \chi_{yy} > \chi_{zz}$ (tetragonal phase). (In the ferroelectric phase, the polar direction is electrically stiffer; this is a well-known feature of ferroelectric perovskites, related to what is usually called "easy polarization rotation"[27].) As can be seen in Supplementary Fig. 4, the three components have an approximate Curie–Weiss behavior, with a maximum at T_C and a monotonic T-dependence on both sides of the transition point.

Figure 1d shows our results for the low-order pyroelectric coefficients. $\pi_z^{(0)}$ is null above the transition point and negative below it, as expected. As for $\pi^{(1)}$, we find the expected behavior as well: the tensor has nonzero diagonal components at all temperatures, nearly diverging at T_C, and changing signs as the system goes through the transition. Note that our numerical

results for $\pi_z^{(0)}$ and $\pi_{zz}^{(1)}$ ratify the competition that occurs when a field is applied parallel to $P_z^{(0)}$, as discussed above. Also, our results for $\boldsymbol{\pi}^{(1)}$ reveal an essentially isotropic tensor at all temperatures, even in the tetragonal phase. (The tetragonal symmetry implies $\pi_{xx}^{(1)} = \pi_{yy}^{(1)} \neq \pi_{zz}^{(1)}$; yet, in Fig. 1d, a sizeable difference between the xx and zz components is found only for $T \lesssim T_C$.)

Figure 1e shows the computed $\Delta T(E_z)$ for various positive fields, with E_z up to 10 MV m^{-1}, as a function of temperature. The results are obtained by evaluating the Taylor series in Eq. (9) up to 5th order, which is enough to get a converged T-change except in the immediate vicinity of the phase transition. More specifically, Fig. 1f shows that, even for a large field of 10 MV m^{-1}, the electrocaloric effect at $T < T_C$ is dominated by the leading contribution $\Delta T^{(1)}(E_z)$, higher-orders becoming significant only very close to T_C (see the result at 490 K). In fact, as shown in Supplementary Fig. 2, we find that the leading contribution to the electrocaloric response—i.e., $\Delta T^{(1)}(E_z)$ below T_C and $\Delta T^{(2)}(E_z)$ above T_C, respectively—is usually a very good approximation of the total effect.

Let us stress that in Fig. 1e, f, we restrict ourselves to fields that are small enough so that no first-order phase transition is induced. This is why we do not show any data very close to T_C, and why the fields considered for $T > T_C$ are relatively tiny. (Close to T_C, the paraelectric phase is easily transformed into the polar one. See representative results in Supplementary Fig. 3.) This is consistent with our perturbative approach to compute $\Delta T(E_\alpha)$, which is designed to describe the properties of the continuously deformed zero-field state. To treat a first-order transition, one could split the integral for $\Delta T(E_\alpha)$ in low- and high-field parts, using different perturbative $\mathbf{P}(\mathbf{E})$ expansions for each of them. In addition, one should account for the latent heat associated with the discontinuous transformation[28–30]. The information to tackle such situations is in principle available from our Monte Carlo calculations. (We can compute latent heat from the thermal-averaged internal energies[31]). However, we should note that, for treating first-order transitions, direct non-perturbative computational approaches based on microcanonical molecular dynamics[8] or constrained Monte Carlo simulations[32] are better suited.

The values obtained for $\Delta T(E_z)$ (e.g., a maximum of 0.25 K when T_C is approached from below for a field of 0.5 MV m^{-1}) are comparable with electrocaloric effects measured for PTO; for example, ref. [33] reports a temperature change of 0.1 K for $T \lesssim T_C$ and a field of 0.15 MV m^{-1}, and a maximum T-change of 1.9 K at T_C. (We also obtain $\Delta S(E_z) \approx -2500$ J K^{-1} m^{-3} for a field of 0.5 MV m^{-1} at $T \lesssim T_C$, while the ref. [33] reports a maximum entropy change of about $-16{,}500$ J K^{-1} m^{-3} for a field of 0.15 MV m^{-1} applied exactly at T_C.) Our results are also consistent with other theoretical estimates of the electrocaloric effect for PTO[34]. Finally, in Supplementary Fig. 5, we evaluate the approximations made in Eq. (9)—i.e., the use of the zero-field values for T and $C_{\mathbf{E}}$, so they can be taken out of the integral—and find that their impact is negligible (even for large fields) except very close to T_C.

Discussion

In view of the above, let us comment on the usual interpretation of electrocaloric effects in terms of field-induced order or disorder. For illustrative purposes, it is convenient to pay attention to the isothermal entropy change, which, from Eqs. (2) and (7), can be written as

$$\begin{aligned}\Delta S(E_\alpha) &= \pi_\alpha^{(0)} E_\alpha + \frac{1}{2}\pi_{\alpha\alpha}^{(1)} E_\alpha^2 + \mathcal{O}(E_\alpha^3) \\ &= \Delta S^{(1)}(E_\alpha) + \Delta S^{(2)}(E_\alpha) + \ldots \\ &= \left(\pi_\alpha^{(0)} + \frac{1}{2}\pi_{\alpha\alpha}^{(1)} E_\alpha + \ldots\right) E_\alpha .\end{aligned} \tag{10}$$

The last line suggests that we can think of $\Delta S(E_z)$ as depending linearly on E_z, the corresponding proportionality constant having spontaneous ($\sim \pi_\alpha^{(0)}$) and field-induced ($\sim \pi_{\alpha\alpha}^{(1)} E_\alpha$) pyroelectric contributions.

Let us consider a ferroelectric state with $P_z^{(0)} > 0$, and imagine we apply an electric field $E_z > 0$. For simplicity (and without loss of generality), let us also assume that the dielectric response is dominated by the linear effect $\chi_{zz}^{(0)}$, higher-order terms being negligible to a good approximation. In such a situation, it is physically sound to assume that the applied field creates order, as it contributes to further align the local electric dipoles in the ferroelectric state and results in a larger order parameter P_z. This field-induced ordering is captured by $\chi_{zz}^{(0)} > 0$, and we know that the effect gets stronger as we approach $T \lesssim T_C$. As a result of this ordering, we expect the entropy to decrease in an isothermal process ($\Delta S(E_z) < 0$), and the temperature to rise ($\Delta T(E_z) > 0$) if the process is adiabatic. These are clear expectations that one would hardly question.

Let us inspect how these expected variations of S and T come about in our formalism. Following the simplification mentioned above (linear dielectric response), we can write $\Delta S(E_z) \approx \Delta S^{(1)}(E_z) + \Delta S^{(2)}(E_z)$. (The discussion for $\Delta T(E_z)$ is analogous.) The first term ($\Delta S^{(1)}(E_z) = \pi_z^{(0)} E_z$) results in a reduction of the entropy, as we have $\pi_z^{(0)} < 0$ for the spontaneous pyroelectric effect. This seems consistent with the ordering argument given above. However, it is important to stress that this term does not contain any information about the dielectric response to the applied field, or about the order the field may create. (There is no generally expected thermodynamic relationship between $\partial P_z/\partial E_z$ and $\partial P_z/\partial T$.) Instead, the entropy change is fully determined by the T-dependence of the spontaneous polarization: $P_z^{(0)} > 0$ decreases as we approach T_C, a behavior that is normal.

The response to an applied field does control the quadratic contribution $\Delta S^{(2)}(E_z)$, where the spontaneous pyroelectric effect in $\Delta S^{(0)}(E_z)$ is replaced by the field-induced one ($\sim \pi_{zz}^{(1)} E_z$). As mentioned above, it is clear that the applied field strengthens the dipole order of the ferroelectric state, as quantified by its order parameter: we have $P_z^{(0)} > 0$ and a field-induced polarization change $\epsilon_0 \chi_{zz}^{(0)} E_z > 0$. However, the corresponding entropy change is positive, since $\pi_{zz}^{(1)} \propto \partial \chi_{zz}^{(0)}/\partial T > 0$ for $T < T_C$. Thus, the same physical mechanism (captured by $\chi_{zz}^{(0)}$) results in field-induced order and a positive contribution to the entropy. Indeed, in what concerns the isothermal entropy change, what matters is not the ordering of the dipoles at a given T. Instead, we have to pay attention to how the field-induced effect changes with temperature. In a ferroelectric state, the ordering caused by the field grows as we heat up towards T_C, that is, we have a positive field-induced pyroelectric effect. This somewhat anomalous behavior (the higher the temperature, the greater the — induced — order) is opposite to the spontaneous pyroelectric effect, and is the one causing $\Delta S^{(2)}(E_z) > 0$ (and $\Delta T^{(2)}(E_z) < 0$).

Hence, the quadratic contribution to the electrocaloric effect in a ferroelectric state, dominated by the linear susceptibility $\chi_{zz}^{(0)}$, seems paradoxical: the field creates order (as quantified by the order parameter) but the entropy increases. The key to the puzzle is that polarization (order) created at a given T is not what controls the entropy; its T-derivative is. This point is hardly new, as it is quite clear from the well-known equations governing electrocaloric effects (Eqs. (1) and (2)); yet, it becomes particularly apparent in our perturbative approach.

Keeping the above in mind, it is easy to interpret the electrocaloric effects in paraelectric and antiferroelectric states, which are dominated by the quadratic contribution. In the paraelectric case, the field-induced order decreases as T increases: at $T > T_C$ we have $\pi_{zz}^{(2)} < 0$, which yields $\Delta S(E_z) \approx \Delta S^{(2)}(E_z) < 0$ and $\Delta T(E_z) \approx \Delta T^{(2)}(E_z) > 0$. It is tempting to interpret this result by focusing on

the response at a given T (the field creates order, hence the entropy should get reduced), but that would not be correct. Instead, the focus should be on the field-induced pyroelectric effect which, in this case, behaves in the normal way, i.e., we have a weaker — induced — order at a higher temperature.

Finally, the inverse electrocaloric behavior of antiferroelectric states is also readily explained within this picture. In that case, we are at $T < T_C$, and have $\Delta S(E_z) \approx \Delta S^{(2)}(E_z) \propto (\pi^{(2)}_{zz} E_z) E_z > 0$ (and $\Delta T(E_z) \approx \Delta T^{(2)}(E_z) < 0$). According to the above discussion, this inverse behavior stems from the fact that the applied field creates polarization more efficiently as T grows toward T_C. Consequently, this disproves the frequent interpretation that the inverse electrocaloric response of antiferroelectric states is caused by field-induced disorder at a given T. As a matter of fact, the above analysis shows that arguments focusing on the field-induced (dis) order at a given T — and overlooking the T-derivative — are incorrect.

To conclude this part, let us comment on a ferroelectric type absent in our discussion: relaxors. As mentioned above (Eq. (1)), ergodicity breaks down in these materials, and the use of the Maxwell relation our formalism relies on is questionable. Nevertheless, some experimental[35] and theoretical[14] reports suggest that, in fact, Eq. (1) approximately captures the electrocaloric response of these systems at a quantitative level; further, it seems to yield qualitatively correct results. Hence, we think that, in the future, it may be worth considering whether our formalism, and the kind of rules summarized in Table 1, might be useful in investigations of relaxors.

In summary, we have introduced a perturbative approach to the electrocaloric effect. This formalism can be applied in quantitative simulation studies, in a straightforward way as long as field-induced (first-order) phase transitions are not present. More specifically, our simulations for ferroelectric $PbTiO_3$ show that, except in the vicinity of the phase transition, a low-order approximation captures the electrocaloric response with great quantitative accuracy. Most importantly, our formalism unifies and clarifies the physical interpretation of all the small-field electrocaloric effects (normal and inverse) observed in ferroelectric and antiferroelectric materials.

Methods

Second-principles simulations. For the second-principles simulations, we used the software called SCALE-UP, which implements the effective-potential approach described in detail in refs. [19,20]. The procedure to obtain this package is described by the developers in [36]. The reader may be interested to know that the same second-principles scheme to simulate lattice-dynamical properties, introduced by Wojdeł et al. in ref. [19], has also been implemented in the package multibinit[37].

As for the visualization and analysis of the simulation data (e.g., for taking numerical derivatives), we used standard free open-source tools that can be readily obtained to run under linux; in particular, much of the work was done using the QtiPlot package[38].

Physical properties from the Monte Carlo simulations. Here, we explain how to compute all the quantities that are relevant in this study—i.e., $\boldsymbol{\chi}$, $\boldsymbol{\pi}$, and $C_{\mathbf{E}}$—from Monte Carlo simulations, at given conditions of temperature and applied electric field. Let us begin with the electric susceptibility,

$$\chi_{\alpha\alpha'} = \epsilon_0^{-1} \frac{\partial \langle P_\alpha \rangle}{\partial E_{\alpha'}}, \tag{11}$$

where α and α' label spatial directions in Cartesian coordinates, and $\langle \dots \rangle$ indicates the thermal average (equilibrium value) as obtained from our Monte Carlo simulations. This thermal average can be written as

$$\langle P_\alpha \rangle = \frac{1}{Z} \sum_i P_{i,\alpha} \exp^{-\beta(U_i - V \mathbf{P}_i \cdot \mathbf{E})}, \tag{12}$$

where Z is the partition function given by

$$Z = \sum_i \exp^{-\beta(U_i - V \mathbf{P}_i \cdot \mathbf{E})}. \tag{13}$$

The sums above run over all the microscopic states of the material, labeled by i; U_i, and P_i are the energy and polarization of state i, respectively; $\beta = (k_B T)^{-1}$, where k_B is Boltzmann's constant and T is the temperature; finally, $\mathbf{E}$ is the applied electric field and V is the volume of the simulated system (as usually done[23], we take the equilibrium volume and assume that volume fluctuations are negligible). Computing analytically the field derivative, we obtain

$$\chi_{\alpha\alpha'} = \frac{\beta V}{\epsilon_0} \left(\langle P_\alpha P_{\alpha'} \rangle - \langle P_\alpha \rangle \langle P_{\alpha'} \rangle \right) \tag{14}$$

Analogously, we can derive the pyroelectric tensor, $\boldsymbol{\pi}$. We have

$$\pi_\alpha = \left(\frac{\partial \langle P_\alpha \rangle}{\partial T} \right)_{\mathbf{E}} = \frac{\beta}{T} \left[\langle U P_\alpha \rangle - \langle U \rangle \langle P_\alpha \rangle \right] \tag{15}$$

where

$$\langle U \rangle = \frac{1}{Z} \sum_i U_i \exp^{-\beta(U_i - V \mathbf{P}_i \cdot \mathbf{E})} \tag{16}$$

is the equilibrium energy. Finally, for the specific heat $C_{\mathbf{E}}$ we have

$$C_{\mathbf{E}} = \frac{1}{V} \left[\left(\frac{\partial \langle U \rangle}{\partial T} \right)_{\mathbf{E}} + \frac{15}{2} N k_B \right], \tag{17}$$

where N is the number of unit cells in the simulation supercell. Here, the first term is related to the potential energy, while the second accounts for the (trivial) kinetic contribution (note we have 3×5 degress of freedom in the five-atom perovskite cell). Calculating the derivative, we finally get

$$C_{\mathbf{E}} = \frac{1}{V} \left[\frac{1}{k_B T^2} \left(\langle U^2 \rangle - \langle U \rangle^2 \right) + \frac{15}{2} N k_B \right]. \tag{18}$$

Computing the adiabatic temperature change. To compute $\Delta T^{(n)}(E_\alpha)$ to arbitrary order (Eq. (9)), we proceed as follows.

$\Delta T^{(1)}(E_\alpha)$ is simply proportional to the spontaneous pyroelectric efffect ($\boldsymbol{\pi}^{(0)}/C_E^{(0)}$, Eq. (9)), which we obtain directly from zero field Monte Carlo simulations, by evaluating the thermal averages as described above.

The higher-order contributions are controlled by field-induced pyroelectricity and can be deduced from the field-dependent susceptibility (see Eqs. (8) and (9)). More precisely, for $T < T_C$, we fit $\chi_{zz} = \chi_{zz}(E_z)$ up to third order in the field E_z, which allows us to compute terms up to $\Delta T^{(5)}(E_z)$ in Eq. (9). For $T > T_C$, we fit $\chi_{zz} = \chi_{zz}(E_z)$ up to fourth order in the field E_z, which allows us to compute terms up to $\Delta T^{(6)}(E_z)$. Supplementary Fig. 1 summarizes the outcomes of this fitting exercise.

Let us note that the slightly different fitting choices, above and below T_C, were adopted in view of the obtained results; in both cases, we tried to push the fit to order as high as possible, while avoiding overfitting. It is also important to keep in mind that, above T_C, the $\chi^{(n)}_{z\dots z}$ terms with odd n are zero by symmetry (i.e., $\chi^{(1)}_{zzz} = \chi^{(3)}_{zzzzz} = \dots = 0$); in turn, this implies that the odd-order terms in the $\Delta T(E_z)$ expansion are also null above T_C.

Finally, we compute numerically (by finite differences) the temperature derivatives of the susceptibility coefficients, and thus obtain the pyroelectric contants $\pi^{(n)}_{z\dots z}$ corresponding to Eq. (7). The $\Delta T^{(n)}(E_z)$ are then trivially calculated.

Representative results for the adiabatic temperature change are shown in Supplementary Fig. 2. It should be stressed that, because our theory is a perturbative one, behaviors associated to discontinuous phase transitions are left out of the fit. A clear example of this occurs at temperatures immediately above T_C, where small fields are able to produce a transformation, as shown in Supplementary Fig. 3. Hence, the computed dielectric constants at 510 K are not fitted at all; and, above that temperature, the fitting range is restricted to small electric fields (see Supplementary Fig. 1).

Data availability

All the relevant data are available from the authors upon reasonable request.

Code availability

The second-principles calculations are carried out using the package SCALE-UP which is proprietary software. Some of the visualizations were done using the free package QtiPlot[38].

Received: 8 December 2020; Accepted: 30 April 2021;
Published online: 09 June 2021

References

1. Kutnjak, Z., Rožič, B. & Pirc, R. Electrocaloric effect: theory, measurements, and applications. in *Wiley Encyclopedia of Electrical and Electronics Engineering* (ed. Webster, J.) 1–19 (John Wiley, Sons, Inc., 2015).
2. Pirc, R., Rožič, B., Koruza, J., Malič, B. & Kutnjak, Z. Negative electrocaloric effect in antiferroelectric $PbZrO_3$. *EPL (Europhys. Lett.)* **107**, 17002 (2014).

3. Geng, W. et al. Giant negative electrocaloric effect in antiferroelectric la-doped $Pb(Zr,Ti)O_3$ thin films near room temperature. *Adv. Mater.* **27**, 3165–3169 (2015).
4. Novak, N. et al. Interplay of conventional with inverse electrocaloric response in $(Pb,Nb)(Zr,Sn,Ti)O_3$ antiferroelectric materials. *Phys. Rev. B* **97**, 094113 (2018).
5. Li, J. et al. Giant electrocaloric effect and ultrahigh refrigeration efficiency in antiferroelectric ceramics by morphotropic phase boundary design. *ACS Appl. Mater., Interfaces* **12**, 45005–45014 (2020).
6. Grünebohm, A. et al. Origins of the inverse electrocaloric effect. *Energy Technol.* **6**, 1491–1511 (2018).
7. Prosandeev, S., Ponomareva, I. & Bellaiche, L. Electrocaloric effect in bulk and low-dimensional ferroelectrics from first principles. *Phys. Rev. B* **78**, 052103 (2008).
8. Marathe, M., Grünebohm, A., Nishimatsu, T., Entel, P. & Ederer, C. First-principles-based calculation of the electrocaloric effect in $BaTiO_3$: A comparison of direct and indirect methods. *Phys. Rev. B* **93**, 054110 (2016).
9. Lisenkov, S., Mani, B. K., Glazkova, E., Miller, C. W. & Ponomareva, I. Scaling law for electrocaloric temperature change in antiferroelectrics. *Sci. Rep.* **6**, 19590 (2016).
10. Marathe, M. et al. Electrocaloric effect in $BaTiO_3$ at all three ferroelectric transitions: anisotropy and inverse caloric effects. *Phys. Rev. B* **96**, 014102 (2017).
11. Glazkova-Swedberg, E., Cuozzo, J., Lisenkov, S. & Ponomareva, I. Electrocaloric effect in $PbZrO_3$ thin films with antiferroelectric-ferroelectric phase competition. *Comput. Mater. Sci.* **129**, 44–48 (2017).
12. Jiang, Z. et al. Electrocaloric effects in the lead-free $Ba(Zr,Ti)O_3$ relaxor ferroelectric from atomistic simulations. *Phys. Rev. B* **96**, 014114 (2017).
13. Kingsland, M., Lisenkov, S. & Ponomareva, I. Unveiling electrocaloric potential of antiferroelectrics with phase competition. *Adv. Theory Simul.* **1**, 1800096 (2018).
14. Jiang, Z. et al. Giant electrocaloric response in the prototypical $pb(mg,nb)o_3$ relaxor ferroelectric from atomistic simulations. *Phys. Rev. B* **97**, 104110 (2018).
15. Moya, X., Kar-Narayan, S. & Mathur, N. D. Caloric materials near ferroic phase transitions. *Nat. Mater.* **13**, 439–450 (2014).
16. Peräntie, J., Hagberg, J., Uusimäki, A. & Jantunen, H. Electric-field-induced dielectric and temperature changes in a 011-oriented $Pb(Mg_{1/3}Nb_{2/3})O_3$-$PbTiO_3$ single crystal. *Phys. Rev. B* **82**, 134119 (2010).
17. Thacher, P. D. Electrocaloric effects in some ferroelectric and antiferroelectric $Pb(Zr,Ti)O_3$ compounds. *J. Appl. Phys.* **39**, 1996–2002 (1968).
18. Li, B. et al. The coexistence of the negative and positive electrocaloric effect in ferroelectric thin films for solid-state refrigeration. *EPL (Europhys. Lett.)* **102**, 47004 (2013).
19. Wojdeł, J. C., Hermet, P., Ljungberg, M. P., Ghosez, P. & Íñiguez, J. First-principles model potentials for lattice-dynamical studies: general methodology and example of application to ferroic perovskite oxides. *J. Phys.: Condensed Matter* **25**, 305401 (2013).
20. García-Fernández, P., Wojdeł, J. C., Íñiguez, J. & Junquera, J. Second-principles method for materials simulations including electron and lattice degrees of freedom. *Phy. Rev. B* **93**, 195137 (2016).
21. Wojdeł, J. C. & Íñiguez, J. Ferroelectric transitions at ferroelectric domain walls found from first principles. *Phys. Rev. Lett.* **112**, 247603 (2014).
22. Gonçalves, M. A. P., Escorihuela-Sayalero, C., García-Fernández, P., Junquera, J. & Íñiguez, J. Theoretical guidelines to create and tune electric skyrmion bubbles. *Sci. Adv.* **5**, eaau7023 (2019).
23. García, A. & Vanderbilt, D. Electromechanical behavior of $BaTiO_3$ from first principles. *Appl. Phys. Lett.* **72**, 2981–2983 (1998).
24. Lines, M. E. & Glass, A. M. Principles and applications of ferroelectrics and related materials. In *Oxford Classic Texts in the Physical Sciences* (Oxford University Press, 1977). https://oxford.universitypressscholarship.com/view/10.1093/acprof:oso/9780198507789.001.0001/acprof-9780198507789.
25. Liu, Y., Scott, J. F. & Dkhil, B. Some strategies for improving caloric responses with ferroelectrics. *APL Mater.* **4**, 064109 (2016).
26. Novak, N., Pirc, R. & Kutnjak, Z. Impact of critical point on piezoelectric and electrocaloric response in barium titanate. *Phys. Rev. B* **87**, 104102 (2013).
27. Fu, H. & Cohen, R. E. Polarization rotation mechanism for ultrahigh electromechanical response in single-crystal piezoelectrics. *Nature* **403**, 281–283 (2000).
28. Tishin, A. M., Gschneidner, K. A. & Pecharsky, V. K. Magnetocaloric effect and heat capacity in the phase-transition region. *Phys. Rev. B* **59**, 503–511 (1999).
29. Giguère, A. et al. Direct measurement of the "giant" adiabatic temperature change in $Gd_5Si_2Ge_2$. *Phys. Rev. Lett.* **83**, 2262–2265 (1999).
30. Sun, J. R., Hu, F. X. & Shen, B. G. Comment on "direct measurement of the 'giant' adiabatic temperature change in $Gd_5Si_2Ge_2$. *Phys. Rev. Lett.* **85**, 4191–4191 (2000).
31. Zhong, W., Vanderbilt, D. & Rabe, K. M. First-principles theory of ferroelectric phase transitions for perovskites: the case of $BaTiO_3$. *Phys. Rev. B* **52**, 6301 (1995).
32. Ponomareva, I. & Lisenkov, S. Bridging the macroscopic and atomistic descriptions of the electrocaloric effect. *Phys. Rev. Lett.* **108**, 167604 (2012).
33. Mikhalevaa, E. A. et al. Caloric characteristics of $PbTiO_3$ in the temperature range of the ferroelectric phase transition. *Phys. Solid State* **54**, 1832–1840 (2012).
34. Lisenkov, S., Mani, B. K., Chang, C.-M., Almand, J. & Ponomareva, I. Multicaloric effect in ferroelectric $PbTiO_3$ from first principles. *Physical Review B* **87**, 224101 (2013).
35. Le Goupil, F., Berenov, A., Axelsson, A.-K., Valant, M. & Alford, N. M. Direct and indirect electrocaloric measurements on $\langle 001 \rangle$-$PbMg_{1/3}Nb_{2/3}O_3$-$30PbTiO_3$ single crystals. *Journal of Applied Physics* **111**, 124109 (2012).
36. "SCALE-UP, an implementation of second-principles density functional theory". https://www.secondprinciples.unican.es/.
37. "Multibinit," https://docs.abinit.org/guide/multibinit/.
38. "QtiPlot, data analysis and scientific visualisation". https://www.qtiplot.com/.

Acknowledgements

We thank E. Defay for many fruitful discussions. Work funded by the Luxembourg National Research Fund through project INTER/RCUK/18/12601980.

Author contributions

M.G. performed the calculations, produced the figures, analyzed the results, and wrote the manuscript. J.Í. supervised the work, analyzed the results, and wrote the manuscript.

Competing interests

The authors declare no competing interests.

Additional information

Supplementary information The online version contains supplementary material available at https://doi.org/10.1038/s43246-021-00167-6.

Correspondence and requests for materials should be addressed to J.Íñi.

Peer review information *Communications Materials* thanks the anonymous reviewers for their contribution to the peer review of this work. Peer reviewer reports are available.

Reprints and permission information is available at http://www.nature.com/reprintsPrimary handling editor: Aldo Isidori.